Educational Administration: Theory and Practice
2024, 30(5), 4495-4505
ISSN: 2148-2403
https://kuey.net/

Research Article

Efficient Classification Of Hyperspectral ImageS Using Multiscale Relation Learning

Antony Vigil M S[1*], Maganti Satya Sai Sathwik[2],Yara Pranav Kumar[3], Lakumarapu Abhishek Kumar[4]

[1*,2,3,4]Department of Computer Science and Engineering, SRM Institute of Science and Technology, Ramapuram, Chennai, India.

Citation: Antony Vigil M S, et.al (2024), Efficient Classification of Hyperspectral Images Using Multiscale Relation Learning, Educational Administration: Theory and Practice, 30(5), 4495-4505
Doi: 10.53555/kuey.v30i5.3652

ARTICLE INFO

ABSTRACT

The classification of hyperspectral images (HSIs) has emerged as a key area of interest in remote sensing and has prompted the investigation of several approaches in recent years. Because of its strong feature extraction capabilities, deep learning has become popular; nevertheless, because of its low discriminative capability, traditional methods frequently produce subpar results. Furthermore, the lack of labelled data makes it difficult to achieve high classification accuracy with small sample sizes in HSI classification. This study suggests a novel method that combines convolutional neural networks (CNNs) with different feature learning techniques to address these problems. The model creates pertinent feature maps for each input feature by feeding a customized CNN architecture with a wide variety of characteristics that are directly retrieved from raw images. These joint feature maps are then used by further layers to forecast final labels for each pixel in the hyperspectral image and this method takes advantage of CNNs' improved feature extraction capabilities while efficiently combining spectral and spatial information to maximize the generated features' discriminative potential. The development of hyperspectral imaging technology, which enables sensors to take pictures in hundreds of bands, highlights the importance of hyperspectral image classification for remote sensing applications. This technology is useful in many different fields, such as monitoring geological disasters, military reconnaissance, monitoring vegetation and ecology, and atmospheric assessment. With multiscale relation learning we have achieved the accuracy rate of 96.13% and 82.6% recall as well.

KEYWORDS: Remote Sensing, Hyperspectral images (HSI), Feature Extraction, Deep learning,

1.INTRODUCTION

A potent multidimensional information acquisition technique for detecting both spectral and spatial information of the Earth's surface is hyperspectral remote sensing. The technology is widely employed in many different industries, including as resource extraction, urbanbuilding, and agricultural monitoring.

A crucial area of study in hyperspectral remote sensing is HSI categorization. Over the last five years, the majority of hyperspectral remote sensing research papers have dealt with classification. The practice of utilizing both spatial and spectral data to assign semantic classes to individual pixels is known as HSI classification. Accurately classifying HSI remains a challenging undertaking for several reasons, despite the rapid development of related research. First, there are non-negligible drawbacks to correct classification resulting from the HSI acquisition method. Aircraft aberrations and alignment variations can also negatively impact imaging; on the one hand, scatteringcan result in spectrum mixing between various classes of nearby image elements. Because of these factors, samples belonging to the same class can occasionally display distinct spectral characteristics, which definitely makes categorization more challenging.

A significant problem limiting classification accuracy is the small quantity oflabeled samples, in addition to the difficulty of classification brought about by the features of HSI itself. The remote sensing community has made extensive use of hyperspectral imagery (HSI) to exploit the hundreds of spectral channels that make up a single scene. However, in order to extract the information from the image, HSI requires reliable andprecise classification systems. Due to the complex nature of the image scene—that is, a lot of data, mixed pixels, and few training samples—the classification of HSI has been regardedas a particularly challenging problem.

Copyright © 2024 by Author/s and Licensed by Kuey. This is an open access article distributed under the Creative Commons Attribution License which permits unrestricted use, distribution, and reproduction in any medium, provided the original work is properly cited.

As a result, numerous attempts have been made to solve this problem over the past few decades. Spectral domain classifiers, including random forest (RF), multinomial logistic regression (MLR), and support vector machines (SVMs), have made significant progress in the early stages of HSI classification.
The latest advancements in technology offer more promising methods for handling HSI classification. For instance, sparsity signal-based techniques (e.g., joint sparse models) and morphological profiles (MPs) were introduced to enhance the comprehension of visual scenes by the use of spatial and contextual features.
These techniques use both spectral and spatial information to try to categorize HSI. A joint sparse model, for example, integrates data from a few test pixel's nearby pixels, which has been shown to be a useful method for enhancing classification performance. With the rapid advancement of Earth observation and imaging technology, there has been a noticeable growth in the use of hyperspectral remote. Through the use of narrow spectral bands, hyperspectral photographs offer abundant information on the land objects. Although the additional dimensionality of the data offers rich information, it presents challenges (the curse of dimensionality) to traditional methods for accurate analysis of hyperspectral pictures, such as classification.
Numerous applications, including target detection, crop categorization, and environmental monitoring, use hyperspectral pictures. Despite the fact that hyperspectral photographs offer extensive and vital information about terrestrial objects, among the hundreds of bands are certain noisy and redundant spectral bands that could cause problems with categorization. It is imperative to employ dimension reduction techniques in order to eliminate these redundancies from the hyperspectral data.
(HSIs) record ground object radiation data across hundreds or even thousands of continuous spectral channels. It is able to acquire spectral properties that capture the distinct qualities of the targets.
HSIs combine the spectral and spatial characteristics of the ground objects, which allows them to capture more subtle variations between them than real photos that simply contain RGB three channels. Because of this benefit, HSIs are very valuable in applications like resource management and usage and environmental monitoring.
It is generally acknowledged in the field of machine learning that the quantity of labeled samples a model has positively correlates with its effectiveness. This is because the model's inadequate capacity to infer regularity from the small sample size leads to a poor generalization ability. It seems sense that having more examples available will probably result in more knowledge that can be learned during classifier training, making it simpler to create a high-performing classifier. Particularly with deep learning's quick advancement, more academics are becoming aware of how crucial a large quantity of labeled data is for model training. It is well known that deep learning models are data-hungry, needing a vast quantity of labeled data in order to fit their massive parameter space.
The abundance of labeled data available is a major factor in the success of deep learning. Even the greatest model could struggle to demonstrate full performance in the absence of enough labeled data. However, in many domains, including hyperspectral remote sensing, getting tagged data is a challenging undertaking. The irreconcilable tension between spectral resolution and spatial resolution typically limits the spatial resolution of high-spatial intensity imaging. Unlike most data labeling in computer vision, the labeling of HSI in this instance cannot be finished only by looking at the photos. Generally speaking, this task needs training samples—the classification of HSI has been regarded as a particularly challenging problem. As a result, numerous attempts have been made to solve this problem over the past few decades. Spectral domain classifiers, including random forest (RF), multinomial logistic regression (MLR), and support vector machines (SVMs), have made significant progress in the early stages of HSI classification.
The latest advancements in technology offer more promising methods for handling HSI classification. For instance, sparsity signal-based techniques (e.g., joint sparse models) and morphological profiles (MPs) were introduced to enhance the comprehension of visual scenes by the use of spatial and contextual features. These techniques use both spectral and spatial information to try to categorize HSI. A joint sparse model, for example, integrates data from a few tests pixel's nearby pixels, which has been shown to be a useful method.

2. LITERATURE SURVEY

In Yigang Tang, Xiaolan Xie, and Youhua Yu's 2022 publication, "Hyperspectral Classification of Two-Branch Joint Networks[1] Based on Gaussian Pyramid Multiscale and Wavelet Transform," they present an effective method for classifying hyperspectral images. This method makes use of Gaussian pyramid multi-scale transformation to collect multi- scale spatial information and wavelet transform to reduce data redundancy in hyperspectral remote sensing. The approach collects spectral characteristics from one branch and multi-scale spatial data from another using a dual-branch feature extraction network. Accurate categorization is made possible by the merging of these information in a complete connection layer, which captures minute nuances and interactions between spectral and spatial variables. Large-scale situations provide issues due to the system's restricted scalability, error-prone nature, and time-consuming nature, notwithstanding its efficacy.
The ear identification technique presented by Matthew Martin Zarachoff, Akbar Sheikh-Akbari[2], and Dorothy Monekosso in their 2022 work, "Non-Decimated Wavelet Based Multi-Band Ear Recognition Using Principal Component Analysis," is quick and effective. The 2D Wavelet based Multi-Band PCA (2D-WMBPCA) technique divides the input picture into sub bands by using a non-decimated wavelet transform.

The technique finds the intersection of the total eigenvector energies and the number of features in each generated frame to get the best matching performance. Each sub band is subjected to normal PCA in order to extract eigenvectors. Experiments conducted on benchmark ear image datasets show that the suggested 2D-WMBPCA strategy outperforms alternative approaches such as eigenfaces and Single Image PCA.

The 2021 paper by Bishwas Praveen and Vineetha Menon presents a deep learning framework for categorization of robust hyperspectral data. The framework achieves better classification performance by effectively combining spectral and spatial information[3]. The system applies supervised classification with a 3-D convolutional neural network, using sparse random projections for spectralfeature extraction and Gabor filtering for spatial feature extraction. The framework performs better in experiments than traditional 2-D CNN-based methods. All things considered, the suggested framework simplifies the process of analyzing hyperspectral data and promises higher classification accuracy for uses in remote sensing. An HSI classification technique based on the weight wavelet kernel JSR ensemble and the -Whale Optimization Algorithm is presented in a work by Mingwei Wang etal[4]. from 2021.

The method makes use of ensemble learning and the wavelet function as the JSR kernel to enable thorough decision-making. The experimental findings provide a 95% overall classification accuracy for hyperspectral pictures, which is outstanding performance compared to previous approaches. The suggested method successfully separates comparable items and gets rid of noise and incorrect categorization. It also adjusts the weights of the sub classifiers to improve classification accuracy.

A SAR image change detection technique based on data optimization and self-supervised learning is presented ina 2020 paper by Wenhui Meng et al. They improve the quality of the first difference image (DI) by using an adaptive gamma correction technique. In order to reduce noise and provide a saliency map for the DI, a novel method based on popular ranking is implemented.

Pre classification accuracy is increased by using the fuzzy[5] local information c-means clustering technique (FLICM) with structural tensor integration. For increased detection accuracy, they train structure maps of the original pictures using convolution wavelet neural networks (CWNN). The experimental findings show better performance than previous approaches, particularly for very noisy SAR photos.

A streamlined 2D-3D CNN architecture for hyperspectral image categorization is presented inChunyan Yu et al.'s 2020 paper. The technique integrates a 2-D CNN with a streamlined 3-D convolution layer to concurrently extract both spatial and spectral data. While the 3-D block[6] reconstructs finer spectral characteristics using information from nearby bands, the 2-D CNN concentrates on extracting rich spectral-spatial properties. The suggested model performs better on widely used testing datasets and successfully increases classification accuracy. Better classification outcomes derive from this strategy's reduction of overfitting and improvement of feature extraction efficiency.

An HSI classification technique based on 2D3D CNN and multibranch feature fusion is presented in a 2020 paper by Zixian Ge et al[7]. By combining 2-D and 3-D CNN, the technique addresses the underuse of interband correlations in HSIs for the extraction of visual information. In the spectral dimension, a multibranch neural network is utilized to extract and combine three different types of information, ranging from shallow to deep. Using popular HSI datasets, the suggested approach outperforms other alternatives in classification performance by utilizing the Mish activation function. Its classification accuracy is marginally less accurate in some datasets than others, though.

A hierarchical clustering-based band selection technique for hyperspectral face identification is presented in a 2019 paper by Qidong Chen et al[8]. The technique reduces duplicate information and mitigates the impact of noise by extracting features using Gabor filters and histograms of oriented gradients (HOG). When compared to alternative techniques, their suggested algorithm, KL-HC-HOG, exhibits reliable performance and temporal economy. In order to improve recognition accuracy, the study highlights the need of effective band selection and recommends more research into sophisticated machine learning algorithms for hyperspectral face recognition. A multi-resolution CNNs framework (MRCNNs) that combines CNNs with ridgelets for extremely high- resolution remote sensing picture categorization is introduced in a 2019 study by Zhifeng Zheng and Jiannong Cao[9].

Trainable convolutional filters extract high-level features, whereas ridgelet filters collect low- level data. These features are then combined to improve CNNs' classification performance. Three VHR remote sensing photos are used to assess the suggested method and show how successful it is in comparison to other methods already in use. The outcomes demonstrate enhanced regional coherence and superior documentationretention, which are especially advantageous for classifying building clusters.

A framework of mixed sparse representations (MSRs) for remote sensing pictures is introduced in a 2017 study by Feng Li et al. to address ill-conditioned situations. The framework represents sub images[10] of smooth, edge-like, and point-like components sparingly via domain transformations. Comparing experimental findings to standard techniques, higher classification accuracy and superior high-resolution picture creation are shown. MSR shows promise as a competitive option for handling a range of ill-conditioned remote sensing issues.

3. PROPOSED MODEL

When the source data is accessible, transfer learning is a potent approach that may help overcome the

problem of small sample sizes and increase training efficiency. On the other hand, virtual samples created from genuine image samples can be used to address the problem of inadequate hyperspectral image (HSI) samples when source data is not available. The total number of training samples is greatly increased by combining these virtual samples with the original ones. When working with support and query sets, mapping modules are used to change the channel dimensionality of either the support or query samples. To confirm the correctness of class prototypes generated from the query samples, each sample is then mixed with another randomly picked sample to create synthetic query samples. This method is done without the use of support samples. The attention mechanism plays a major role in improving feature discrimination and is widely used in HSI classification, especially in convolutional neural networks (CNNs). Rich spectral and spatial information may be extracted from hyperspectral pictures, and doing so well is essential for precise categorization. In order to investigate the long-distance interactions between spatial dimensions and the variations in spectral band relevance, a coordinated attention mechanism is developed. Based on these correlations, this process produces spectral and spatial attention masks.

CNNs are very good at extracting features, especially by using techniques like pooling and convolution that provide more insight into the input data. CNNs are able to prevent data loss by maintaining the correlation between data pixels because of the characteristics of HSIs. In HSI classification, efficient spatial and spectral information extraction is still crucial. Pretraining involves training the proposed network using two source HSI datasets, the Salinas and Pavia Center datasets, which include the greatest number of labeled samples among publicly available HSI datasets.

The model is pretrained for N epochs after being initialized with a Gaussian distribution on a single-source HSI dataset. The feature extraction portion is then fixed, and a Gaussian distribution is used to reinitialize the classifier. Next, the classifier on the other source HSI dataset and the feature extraction portion are pretrained for N/2 epochs at a different learning rate. The whole model—aside from the classifier—is transferred to initialize the target HSI dataset after pretraining on the two source datasets. For training the second source HSI dataset, the transfer component and the new classifier are optimized at the same learning rate.

Comparing the suggested method to the most recent approaches, extensive trials show that it delivers state-of-the-art performance. Moreover, the method maintains a comparable performance in the target tasks with only a small number of labeled samples while pretraining on existing datasets, which broadens its applicability to a variety of domains. A straightforward dimensionality reduction technique is suggested to preserve uniform input data dimensions without the need for labeled samples from the HSIs in order to promote transfer learning. In order to guarantee that the number of bands in the source and target data is the identical, this technique involves choosing bands from the original HSI datasets.

In conclusion, the suggested approach seeks to improve the prototype network's robustness in HSI boundary pixel classification. This work's primary contributions include the creation of a technique for arbitrarily combining two HSI patches, the emulation of boundary patches, and the use of synthetic patches to improve training data for few-shot HSI classification. Using a transformer as a feature extractor to pay varied attention to different pixels and enhance label generation for synthetic patches, a lightweight prototype network is created for online patch mixing.

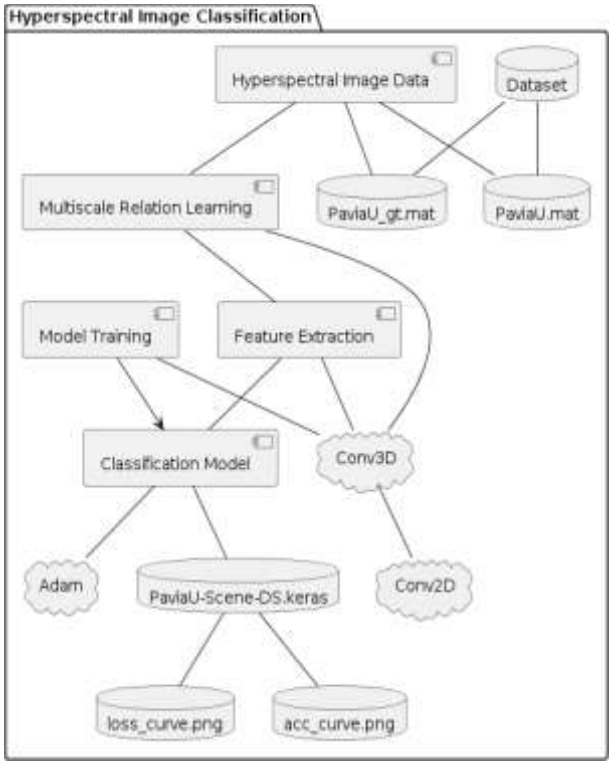

Fig 1. Architecture Diagram of Proposed Model

4.METHODOLOGY

4.1: Multiscale Blocks

The Multiscale Blocks structure with a channel attention module is meant to extract and choose spectral information. in order to fully extract noteworthy spectrum properties. The second phase uses the dense connection structure to appropriately extract the information and extract additional spectral attributes.The structure of the first convolution layer, which has a 3D-The soft pool module is used to extract additional spatial data, widen the receiving field of a subsequent convolution, and improve classification performance. In addition, several optimization strategies are used to prevent overfitting. A spectral attention mechanism is incorporated into each branch to generate spectral features that are more conducive to grouping. The spectral properties of four branches are then aggregated.

In the second step, which is based on the Dense Net structure and the idea of recycling spectral characteristics, the fused features are inserted into the Dense Net. Dense blocks with three convolution layers are used to extract spectral and network properties. The third segment and the extraction of spectral features are similar. The original hyperspectral data is received by a dense block that contains a three-dimensional soft pool. The 3D-Softpool module is used to improve the first convolution layer of dense blocks. In order to extract spatial attention mechanism and spatial neighborhood features. Following element-by-element addition of the feature maps derived from the spectral and spatial branches.

4.2 Spectral Self-Attention

The first part consists of the proposed Multiscale Blocks structure with spectral self-attention mechanism. First, principal component analysis (PCA) is applied to the original hyperspectral picture data. $P \in R$ pow(9×9×band), where 99 is the length and breadth of the data and band is the number of channels, is the remaining data after PCA. Next, a three-dimensional convolution operation is carried out on the data $P \in R$ pow(9×9×band). The convolution kernel size of the three-dimensional convolution layer is set to (1 1 7), the padding to (0 0 0), and the stride to (1 1 2). With this method, the length and breadth of the data, as well as the number of channels, become an, meaning that an is the number of channels of the data following the convolution layer operation.

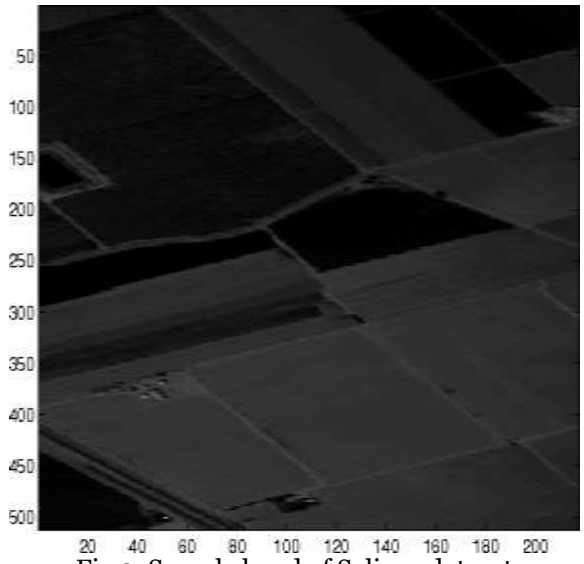

Fig 2: Sample band of Salinas dataset

The four branches of the Multiscale Block module receive the output data concurrently, and each branch works to maintain as much of the important spectrum information as possible thanks to the spectral self-attention mechanism.
The first branch of the Multiscale Blocks module uses convolution using the convolution layers with six convolution kernels. To ensure consistency in the amount of the input and output data, the population approach is applied to all branches. The batch normalization (BN) layer is employed after the convolution layer. To hasten the model's convergence, the BN layer has the ability to normalize and scale the channel linearly.

4.3 Multiscale Relation Learning Network

Six convolution kernels, each having a size of (111), areused in the first convolution layer, together with BN + Mish. Six convolution kernels with a size of (337) are used in the second convolution layer, together with BN+ Mish. At the end of the second branch, spectral self- attention is used with an input size of (9*9*a). Despite having the identical structure, the third and fourth branches have distinct convolution kernel sizes. Three (3*3*7) sized convolution kernels make up the third branch's total of six convolution kernels. There are six convolution kernels in total, with the fourth branch's convolution kernel size being (5*5*7).
After the convolution layer, BN + Mish and the spectral self-attention approach are applied to avoid data explosion and gradient disappearance. Since data padding is used in all four branches, the output
size is (9*9*a,6). The cube size that results from adding up the data outputs from the four branches is (9*9*,24).
The Multiscale Blocks module's cube output has a wealth of relevant spectral feature information that provides rich spectral feature information for subsequent operations. The dense connection network is a crucial network for the second and third parts of the proposed approach. In order to avoid the gradient disappearance issue brought about by the depth of the Multiscale Blocks module, the dense connection module is utilized behind it to further extract the useful spectral features. The network's tiers are all directly linked in order to ensure full information flow between the intermediate layers.

Dataset description

The ROSIS sensor collected the hyperspectral Pavia Center dataset while conducting a flying campaign over Pavia, northern Italy. For Pavia Centre, there are 102 spectral bands. The picture Pavia Centre is 1096 by 1096 pixels. There is a 1.3-meter geometric resolution. Nine classes are distinguished by image ground truths each. Prof.Paolo Gamba of the Telecommunications and Remote Sensing Laboratory at Pavia University (Italy)contributed the sceneries from Pavia.

Table 1: Comparative performance of the model with optimization and with Multiscale relation approach

Metric	With optimization	Without optimization	P-Value
Accuracy	96.13%	94.12%	0.0048
Precision	82.68%	91.43%	0.0024
Recall	82.50%	69.92%	0.0000
F1-score	83.92%	77.63%	0.0003

Table 1. Shows a quantitative perspective, using optimization learning has shown significant improvements in a range of performance indicators. Notably, the system's accuracy in the crucial area of intrusion detection

has increased from 94.12% to 96.13%, demonstrating a noteworthy, although relatively little, gain. In addition, the recall rate has increased significantly from 69.92% to 82.50%, indicating a higher capacity to identify real threats, which is critical for protecting critical infrastructure. The precision decreased slightly, from 92.43% to 87.68%, but overall, the balance between accuracy and review has improved, as indicated by the F1 score. 0.0024, 0.0000, and 0.0003, in that order, supporting the notion that enhancement learning has a noteworthy impact on the framework's display metrics. Get a dataset ready so the LSTM network may be trained. Create sequences that symbolize possible solutions, then calculate the values of the relevant goal functions for each sequence. Divide the dataset into sets for validation and training. Utilizing the prepared dataset, train the LSTM model by fine-tuning the network weights to precisely forecast the values of the goal function. Keep an eye on the training process to avoid overfitting and guarantee convergence. Use the trained LSTM model to produce sequences that could be possible answers to the optimization issue. Sequences that are generated should show patterns that were picked up during training. Make sure the resulting sequences follow any optimization problem requirements by post-processing them. Put limitations management strategies into practice and adjust the solutions as necessary.
Utilizing the objective function, assess the created solutions. To enhance the quality of the answer, iterate by modifying the parameters or the LSTM model as needed. Optimize hyperparameters and fine-tune the LSTM model to improve the multiscale relation learning algorithm's performance.

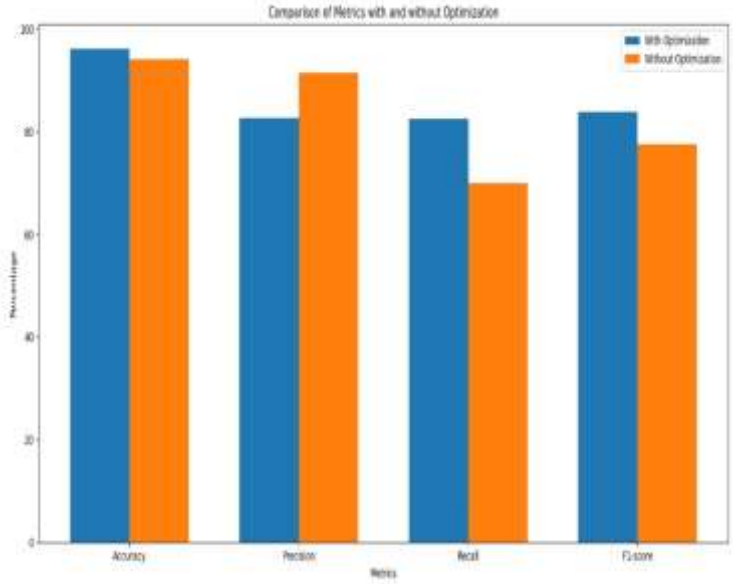

Fig 3: comparison of metrices with and without optimization

From a quantitative perspective, as shown in Figure 3, integrating optimization learning has led to significant improvements in a number of performance indicators.

5. RESULTS AND DISCUSSION

In order to assess the effectiveness and efficiency of our suggested approach, we conducted a comparable analysis using standard metrics in this domain: Real Benefits (TP): Handles attack events that are correctly identified by the Interruption Discovery Framework (IDS). Real Negatives (TN): Shows typical occurrences that the IDS has appropriately categorized. Bogus Up-sides (FP): Refers to common occurrences that the IDS mistakenly identified as attacks. False Negatives (FN): Indicates attack events that the IDS is unable to distinguish. Additionally, the following measurements were used for evaluation: Identification rate (DR): The Discovery Rate (DR) computes the ratio of the total number of occurrences to the number of occurrences that are appropriately classified. It considers both positive and negative instructions when examining the hit rate of the suggested security solutions. The DR is shown in Condition 2, where the quantity of positive and negative findings across all arrangements—including fraudulent pros and cons are taken into consideration. The ratio of all instances assigned as positive to misleading positive sides is known as the Bogus Positive Rate (FPR). The ratio of all examples delegated negative to misleading negatives is known as the Bogus Negative Rate (FNR). It assesses instances in which a request is identified as an attack even when the stream was a typical request or access.

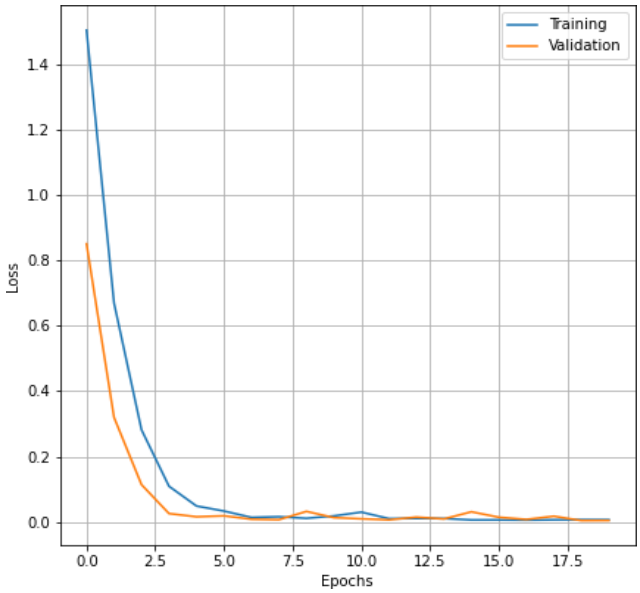

Fig 4: Plotting of loss vs epoch for train and test

In Fig :4, A deep learning model is essentially being observed as it learns throughout a sequence of epochs, or iterations, when the training and validation process is represented graphically on a graph. The number of times the model has iterated across the whole training dataset is displayed on the x-axis, which represents the epochs. The model adjusts its parameters at each epoch in an attempt to improve the model's fit to the training set, which should have the capacity to reduce the loss of it. The loss, or how well the model's predictions match the actual labels, is plotted on the y-axis. As the model gains knowledge from the training data, the loss should ideally decrease during training. This decline suggests that the model's forecast accuracy is increasing. But it's important to keep an eye on both the training and validation losses. The model's performance on a different validation dataset—one that it was not exposed to during training—is gauged by the validation loss.

This is a stand-in for the model's capacity to generalize to previously undiscovered data. Overfitting of the model is indicated if the training loss keeps decreasing but the validation loss starts to grow. When a model grows too complicated and begins to learn specific patterns from the training set rather than general ones, this is known as overfitting. It consequently does well on training data but badly on fresh, untested data.

In Fig: 5, The x-axis displays the epochs, while the y-axis displays the accuracy. Iterations across the complete training data set are called epochs. The training accuracy is shown by the red line, while the validation accuracy is shown by the blue line.

As the number of epochs increases in the graph, so does the training accuracy. This indicates that the model is effectively assimilating the training set.

Table 2: Comparative analysis of our work with other methods

S.No.	ML Algorithm	Precision-Recall Score	ROC - AUC Score	F-1 Score
1.	Isolation forest	91%	94%	81%
2.	Support Vector Classifier	76%	94.5%	80%
3.	XGBoost Classifier	92.2%	96.3%	93%
4.	Multiscale relation model	96%	95.2%	95.2%

Isolation Forest: With a Precision-Recall Score of 91%, this algorithm is 91% accurate in its predictions of positive outcomes. The algorithm appears to perform effectively in differentiating between positive and negative cases, as indicated by the ROC - AUC Score of 94%. The balance between recall and precision is shown by the F1 Score of 81%; a higher number denotes greater performance.

Support Vector Classifier: This method performed less precisely than Isolation Forest, with a Precision-Recall Score of 76%. It did, however, obtain a higher ROC - AUC Score of 94.5%, suggesting improved class discrimination. The F1 Score of 80% indicates that memory and precision are fairly balanced. XGBoost Classifier: This method showed a high degree of precision in predicting positive instances, as seen

by its Precision-Recall Score of 92.2%. Excellent discrimination ability is suggested by the ROC - AUC Score of 96.3%, and a great balance between precision and recall is indicated by the high F1 Score of 93%.

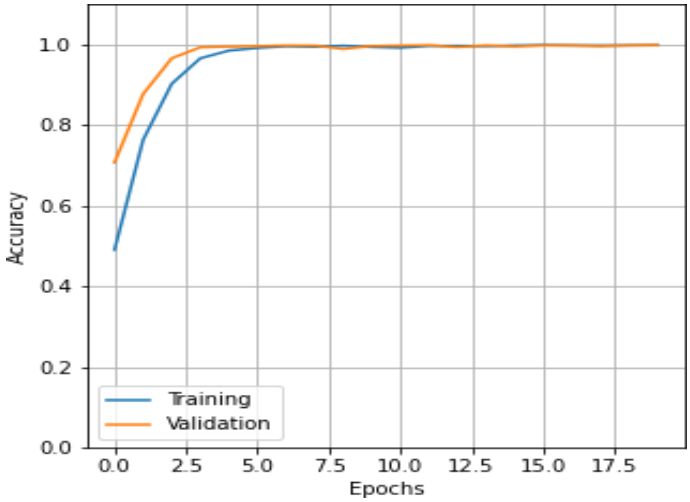

Fig 5: Plotting of accuracy vs epoch for train and test

Multiscale Relation Model: This approach proved to be the most accurate in predicting positive cases, achieving the maximum Precision-Recall Score of 96%. With a ROC - AUC Score of 95.2%, the XGBoost Classifier-like performance in discrimination is suggested. It also achieved an F1 Score of 95.2%, which is similar to XGBoost Classifier and shows a good balance between precision and recall.

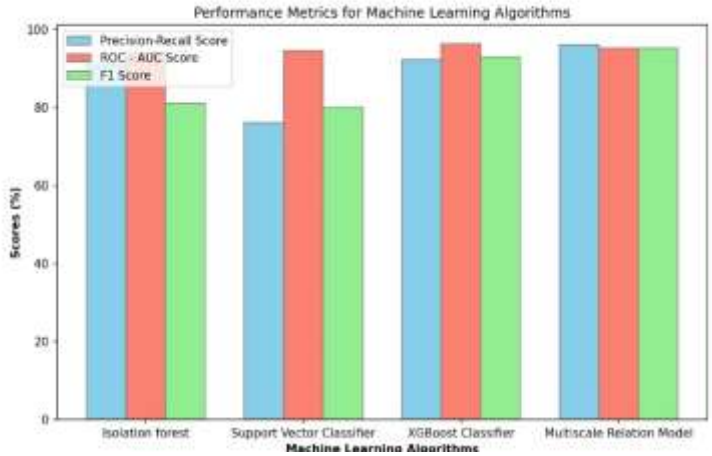

Fig 6: Comparative analysis of proposed work with other works

6. CONCLUSION

The Multiscale Blocks module, 3D-Soft pool module, spatial attention module, channel attention module, and dense connection are all used in this method's network structure. With the Multiscale Blocks module, the spectrum properties of hyperspectral images may be obtained at several scales and levels. In order to filter out extraneous information and obtain more meaningful data, the spectral attention module is introduced to every Multiscale Block branch. Whenemploying a thick connection structure, spatial featuresmay be directly cut from several layers, enabling feature reuse and improving feature extraction efficiency. To tackle the problems caused by a dearth of annotated datasets, a simple yet much more complex architecture was proposed. The ability of deep learning to extract representative characteristics may be leveraged by this architecture. Second, the proposed AI Unit considers the properties of hyperspectral images and gives priority to spectral fingerprints over geographical settings. Moreover, a data-fusion transfer learning strategy is applied to improve the initialization and classification accuracy of the model.

7. FUTURE WORK

In order to completely use the spectrum and spatial features at the edge to classification, we will investigate in more detail how to fuse the retrieved spatial-spectral features more successfully in future study. As a result, developing a fusion model that is more effective is a crucial area for our future study.

REFERENCES

1. Farhan Ullah,Yaqian Long,Irfan Ullah,Rehan Ullah Khan,Salabat Khan, Khalil Khan, Maqbool Khan, Giovanni Pau Deep Hyperspectral Shots: Deep Snap Smooth Wavelet Convolutional Neural Network Shots Ensemble for Hyperspectral Image Classification IEEE Journal of Selected Topics in Applied Earth Observations and Remote Sensing, 2023
2. Yigang Tang,Xiaolan Xie,Youhua Yu Hyperspectral Classification of Two-Branch Joint Networks Based on Gaussian Pyramid Multiscale and Wavelet Transform IEEE Access, 2022
3. Mingwei Wang,Zitong Jia,Jianwei Luo,Maolin Chen,Shuping Wang,SZhiwei Ye A Hyperspectral Image Classification Method Based on Weight Wavelet Kernel Joint Sparse in Applied Earth Observations and Remote Sensing, 2021
4. Matthew Martin Zarachoff,Akbar Sheikh- Akbari,Dorothy Monekosso Non-Decimated Wavelet Based Multi-Band Ear Recognition Using Principal Component Analysis IEEE Access, 2021.
5. Qidong Chen,Jun Sun,Vasile Palade,Xiaoqian Shi,Li Liu Hierarchical Clustering Based Band Selection Algorithm for Hyperspectral Face Recognition IEEE Access, 2019
6. Zhifeng Zheng,Jiannong Cao Fusion High-and-Low- Level Features via Ridgelet and Convolutional NeuralNetworks for Very High-Resolution Remote Sensing Imagery Classification IEEE Access, 2019.
7. Bishwas Praveen, Vineetha Menon Study of Spatiala Spectral Feature Extraction Frameworks With 3-D Convolutional Neural Network in 2020
8. Feng Li, Lie Xin, Yi Guo, Junbin Gao, Xiuping Jia A Framework of Mixed Sparse Representations for Remote Sensing Images IEEE Transactions on Geoscience and Remote Sensing, 2016 Wenhui Meng, Liejun Wang, Anyu Du, Yongming Li SAR Image Change Detection Based on Data Optimization and Self-Supervised Learning IEEE Access 2020.
9. Chunyan Yu, Rui Han, Meiping Song, Caiyu Liu, Chein-I Chang A Simplified 2D-3D CNN Architecture for Hyperspectral Image Classification Based on Spatiala Spectral Fusion IEEE Journal of Selected Topics in Applied Earth Observations and Remote Sensing, 2020.
10. Zixian Ge, Guo Cao, Xuesong Li, Peng Fu Hyperspectral Image Classification Method Based on Spatiala Fusion and 2D-3D CNN and Multibranch Feature Fusion IEEE Journal of Selected Topics in Applied Earth Observations and Remote Sensing,2020.
11. X. Jia, B.-C. Kuo and M. M. Crawford, Feature mining for hyperspectral image classification, Proc. IEEE, vol. 101, no. 3, pp. 676-697, Mar. 2013.
12. P. Ghamisi et al., Advances in hyperspectral image and signal processing: A comprehensive overview of the state of the art, IEEE Geosci. Remote Sens. Mag., vol. 5, no. 4, pp. 37-78, Dec. 2017.
13. S. Roessner, K. Segl, U. Heiden and H. Kaufmann, Automated differentiation of urban surfaces based on airborne hyperspectral imagery, IEEE Trans. Geosci. Remote Sens., vol. 39, no. 7, pp. 1525-1532, Jul. 2001.
14. G. Camps-Valls, D. Tuia, L. Bruzzone and J. A. Benediktsson, Advances in hyperspectral image classification: Earth monitoring with statistical learning methods, IEEE signal Process. Mag., vol. 31, no. 1, pp. 45-54, Jan 2014.
15. J. Li, I. DÃ³pido, P. Gamba and A. Plaza, Complementarity of discriminative classifiers and spectral unmixing techniques for the interpretation of hyperspectral images, IEEE Trans. Geosci. Remote Sens., vol. 53, no. 5, pp.2899-2912, May 2014.
16. Y. Yuan, Y. Feng and X. Lu, Projection-based NMF for hyperspectral unmixing, IEEE J. Sel. Topics Appl. Earth Observ. Remote Sens., vol. 8, no. 6, pp. 2632-2643, Jun. 2015.
17. W. Li, Q. Du and B. Zhang, Combined sparse and collaborative representation for hyperspectral target detection, Pattern Recognit., vol. 48, no. 12, pp. 3904-3916, 2015.
18. X. Huang and L. Zhang, An SVM ensemble approach combining spectral structural and semantic features for the classification of high-resolution remotely sensed imagery, IEEE Trans. Geosci. Remote Sens., vol. 51, no. 1, pp. 257-272, Jan. 2012.
19. H. Goldberg, H. Kwon and N. M. Nasrabadi, Kernel eigenspace separation transform for subspace anomaly detection in hyperspectral imagery, IEEE Geosci. Remote Sens. Lett., vol. 4, no. 4, pp. 581-585, Oct. 2007.
20. V. Sharma, A. Diba, T. Tuytelaars and L. Van Gool, Hyperspectral CNN for image classification & band selection with application to face recognition, 2016.
21. S. Veraverbeke et al., Hyperspectral remote sensing of fire: State-of-the-art and future perspectives, Remote Sens. Environ., vol. 216, pp. 105-121, 2018.
22. MS Antony Vigil, V Subbiah Bharathi, Classification of periodontitis stages in mandibular area from dental panoramic radiograph using adaptive centre line-distance based image processing approach, Journal of Ambient Intelligence and Humanized Computing, vol. 14, pp. 8859-8869, published by Springer Berlin Heidelberg, cited by 3, 2023.
23. Antony Vigil, Aashna Chib, Ayushi Vashisth, Tanisha Pattnaik, DETECTION OF CLOUD SHADOWS USING DEEP CNN UTILISING SPATIAL AND SPECTRAL FEATURES OF LANDSAT IMAGERY, Computing Technology Research Journal, vol. 1, pp. 22-29, cited by 2, 2022.

24. Harrish P M.S.Antony Vigil, Selva J, Time Series Modelling and Domain specific predicting air passenger flow traffic using Neural Network, International Journal of Special Education, vol. 37, pp. 15023-15037, published by SPED, cited by 2, 2022.
25. MS Antony Vigil, M Mirutuhula, Sure Sarvagna, R Supraja, Gadusunari Priyanka Reddy, DNA Sequencing Using Machine Learning Algorithms, 2022 International Conference on Data Science, Agents & Artificial Intelligence (ICDSAAI), vol. 1, pp. 1-4, published by IEEE, cited by 1, 2022.
26. V Subbiah Bharathi M S Antony Vigil, Detection of periodontal bone loss in mandibular area from dental panoramic radiograph using image processing techniques, Concurrency and Computation: Practice and Experience, published by Wiley, cited by 9, 2021.